BUILD SIMUL (2019) 12: 129–140
https://doi.org/10.1007/s12273-018-0487-z

Daylight luminous environment with prismatic film glazing in deep depth manufacture buildings

Zhen Tian[1] (✉), Yaping Lei[2], Jacob C. Jonsson[3]

1. School of Architecture, Soochow University, Suzhou, China
2. Suzhou Institute of Building Science Group, Suzhou, China
3. Lawrence Berkeley National Laboratory, Berkeley, CA 94720, USA

Research Article

Building Thermal, Lighting, and Acoustics Modeling

Abstract

In this paper, indoor illuminance distributions with a microstructured prismatic film glazing in a deep depth manufacture space were measured. The measured illuminance data with the prismatic film glazing were compared to Radiance simulation results with a conventional glazing. This study shows that using prismatic film glazing at side windows can improve indoor illuminance levels and illuminance uniformity for inner spaces. The technology can work effectively for deep depth manufacture spaces under a clear sky but less effective under an overcast sky for improving illuminance levels and illuminance uniformity. Luminance image and glare metrics were also compared between the prismatic film glazing and conventional glazing. The angle-dependent transmittance properties of light-scattering for the prismatic films with direct sunlight present a different luminance pattern from the conventional glazing with higher peak luminance values but smaller peak luminance areas. In general, the simulated glare metrics with the prismatic film glazing presented lower DGP and DGI glare index than those with the conventional glazing. The time and orientation which may cause high glare metrics and possible discomfort glare with the prismatic film glazing in the deep depth manufacture space are also discussed.

Keywords

luminous environment,
manufacture buildings,
illuminance uniformity,
luminance,
glare metrics

Article History

Received: 25 June 2018
Revised: 20 September 2018
Accepted: 11 October 2018

1 Introduction

Daylight is essential to indoor occupant well-being and has great potential for building energy savings if deployed effectively (IEA 2000; Heschong Mahone Group 2002). In the past twenty years, the value of daylight has regained recognition and popularity, with the developing innovative technology and fast growing green building markets. In general, there are primarily two ways of employing daylight: skylights and side windows. While skylights are mainly applied in atriums, lobbies and underground spaces, side windows have much wider applications combined with view function. Limited by the aperture parameter factors such as size, shape and position, providing good daylight for deep depth spaces, e.g. manufacture spaces through side-windows presents a challenge.

A number of studies have been devoted to the development of products and technologies that can redirect direct sunlight and diffuse light into the building's deeper space, aiming to increase the daylit area and also to improve the uniformity of side-window daylighting. These products and technologies include light shelves, Anidolic, Retrolux blinds, microstructured prisms, etc. (Beltrán et al.1997; IEA 2000; Scartezzini and Courrct 2002; RETROSOLAR 2014; 3M 2017).

Among the light-redirecting systems, the prismatic film glazing has drawn attention recently. A prismatic film glazing at side windows can refract and reflect light to ceiling, then to the inner spaces from ceilings, providing the opportunities to improve indoor illuminance environment. The mechanism of prismatic film glazing is a microstructured saw-tooth prismatic film inserted between double glazing unit (surface #2 or #3) or adhered to the inside surface of a glazing (surface #4), so that sunlight passing through a prismatic film glazing at side windows will be majorly refracted upward to the ceiling (Fig. 1) and then be reflected downward from ceiling to the inner spaces. In side window application, the

E-mail: tianzhen@suda.edu.cn

daylit area can be increased and illuminance levels at inner spaces may be improved. As to the angle-dependent transmittance and reflectance properties of light-scattering for prismatic film, the incoming sunlight angle (solar altitude angle) plays an important role affecting the outgoing light scattering distribution. Under certain conditions, for example, when the solar altitude is low, (i.e. 9:00 and 15:00 for east and west side windows), the redirection light has a low outgoing angle and downward peak flux (Fig. 2) and may possibly result in glare issues, depending on the position, structure, and shape of the microstructure saw-tooth prisms.

International Energy Agency (IEA) Solar Heating and Cooling Program Task 21, Annex 29 Subtask A: Performance Evaluation of Daylighting Systems (IEA 2000) has provided several case studies with applied prismatic panel or film systems for daylighting and/or solar shading. Thanachareonkit and Scartezzini (2010) compared daylighting performance results of Complex Fenestration System (CFS) including prismatic panel systems with physical and virtual simulation

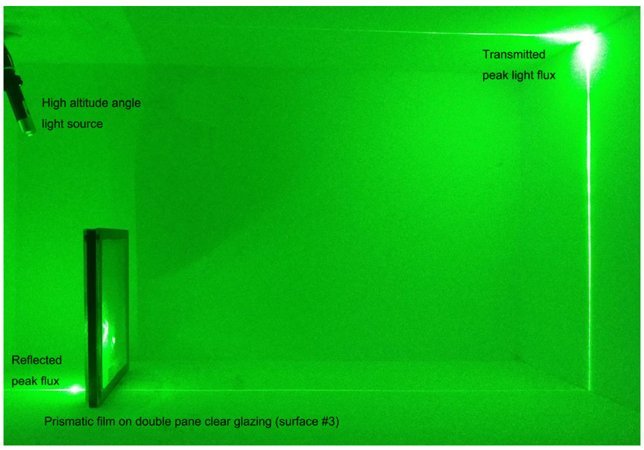

Fig. 1 Light transmittance properties through prismatic film with clear glazing (high altitude angle)

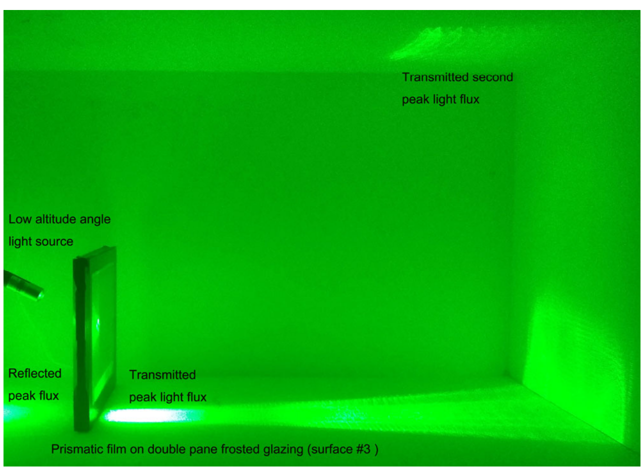

Fig. 2 Light transmittance properties through prismatic film with frosted glazing (low altitude angle)

models, and proposed guidelines to avoid or estimate errors for CFS daylighting performance analysis. McNeil et al. (2017) studied the daylight performance with a 3M prismatic film product through detailed simulation and found that lighting energy saving possibility can reach 40% for a south facing, 12 m office space. Mashaly et al. (2017) have studied the daylight environment performance with prismatic panel windows and the research revealed the daylight autonomy can be improved 25%–34% compared to a conventional glazing for an 8.1 m depth small-scale prototype test space under southern skies.

As different manufacturers may produce specific shape, size and configuration of prismatic film products for solar shading and/or daylighting, the light scattering properties of different prismatic film products need to be analyzed. Researchers have developed Bidirectional Scattering Distribution Function (BSDF) method to study the light scattering and distribution properties of prismatic film glazing (Asmail 1991), and the impact on building daylight luminous environment. In the Radiance program, the genBSDF tool can generate BSDF files based on different products parameters (Ward et al. 2011). Meanwhile, a method for laboratory measuring prismatic film light scattering properties was developed (Andersen et al. 2003; Andersen 2004), which became a useful laboratory testing and measuring procedure for BSDF materials.

2 Prismatic film glazing application in deep depth factory buildings

2.1 Daylight case study building

Large factory buildings usually have high ceilings and deep depths with the manufacture requirements. The pattern of manufacture buildings commonly leads to difficulties in utilizing daylighting effectively through conventional side windows, but it may provide a good opportunity for prismatic film glazing application.

Previous research of the prismatic film glazing majorly studied the space daylight performance with south facing windows (IEA 2000; McNeil et al. 2017). Meanwhile, the luminance performance with prismatic film glazing in high-ceiling and deep-depth spaces such as manufacture spaces is rarely studied and reported. This research focused on the daylight performance analysis with the prismatic film glazing in deep depth manufacture buildings, under both clear and overcast skies while the latter were seldom investigated.

The three-floor Suming Decoration Company Office Building (Figs. 3 and 4) is utilized as the study case. The Building's ground floor is the assembly factory space, with 9 meters in ceiling height, 40 meters in width (west-east

Fig. 3 Exterior view of the Suming Decoration Building

Fig. 4 Interior view of the first floor in the Suming Decoration Building

direction) and 55 meters in length (north-south direction). All the ground floor side windows are 3.1 meters in sill height and each window is 1.9 meters high. To improve the deep-depth space daylighting illuminance levels and reduce possible glare, a prismatic film with frosted glazing were installed on the East, West and South elevation windows of the ground floor.

In the Suming Decoration Building, to reduce the chromatic dispersion phenomenon with the light passing microstructure prism, the prismatic film glazing units were placed the saw-tooth prisms facing the incident sunlight than the contrastive arrangement, while the latter is usually how the 3M products applied and also in other application setup (IEA 2000). Meanwhile, to reduce possible strong outgoing light flux and glare with the prismatic film, a diffuse layer can be applied, including diffusing film, frosted glazing or obscure glazing can be combined with the prismatic film even though the diffuse layer may reduce the total daylight flux into spaces (Fig. 2).

2.2 Prismatic film glazing light characteristics and laboratory test

The micro structure of the prismatic film tested with a laser microscope 3D profile measurement is presented in Fig. 5. The micro prism dimension is around 46 μm in height and 30 μm between two prisms. Meanwhile, there is a chamfering in the top with the angle of 57°. The prismatic film structure properties have important impact on the light transmittance, reflection, scattering characteristics. The laboratory test method of the prismatic film properties

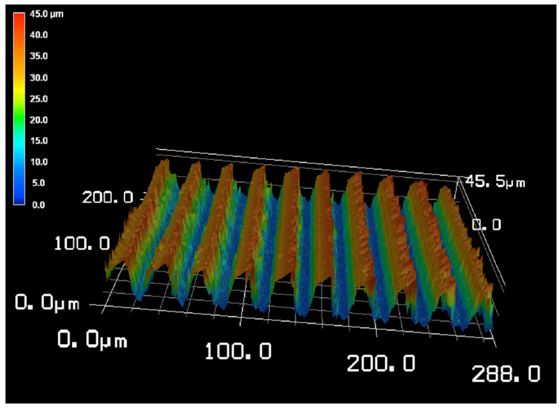

Fig. 5 Microstructure of the prismatic film used in the Suming Decoration Building

with goniophotometric measurements was used with higher accuracy representation of the microstructure to generate synthetic BSDF data for the light characterization than using the back ray-tracing genBSDF tool. A 30 cm × 30 cm prismatic film plus frosted double glazing unit sample was tested in the Lawrence Berkeley National Laboratory with a goniophotometric. The configuration of the double glazing units is the 5 mm fabric surface glazing plus 5 mm clear glazing with the prismatic film on surface #3 and saw-tooth prisms facing the incident light. In this configuration, possible glare and chromatic dispersion effects can be reduced, compared to a clear glazing and saw-tooth prisms facing inside configuration.

Similarly to test method in the research by McNeil et al. (2017) but with adjustment in test angle, a total of eighteen angles of incidence were measured: (a) nine for phi $\varphi_i = 90°$ (plane normal to the sample glazing) with θ_i ranging from 0° to 82.5° at 10° increments, except the last increment of 12.5°, and (b) nine for $\varphi_i = 45°$ for the same set of θ_i angles.

A halogen tungsten lamp was used as the light source which illuminated a 2.5 cm diameter region of the test sample (more than 10 periods of the microstructure) at normal incidence. Detector measurements were made at a uniform angular resolution of 1° over the entire hemisphere with finer resolution sampling around the peaks.

To describe the relationship between the light incident angle and outgoing flux scattering distribution in respect to complex fenestration systems (CFS) including the prismatic film material, Lawrence Berkeley National Laboratory has developed the BSDFViewer tool (LBNL 2017). BSDFViewer tool can visualize light incident hemisphere and flux transmission as well as reflection hemisphere for BSDF materials. Each of the incident, reflectance and transmission hemispheres is divided into different patches. According to the methods of dividing patches, two types of files, i.e. Klems and Tensor Tree data files (Klems 1994a,b; McNeil et al. 2013), can be created within Radiance program or through goniophotometric measurement, and presented the results with BSDFViewer, while the BSDFViewer for Tensor Tree data can only be presented at the Mac OS platform. Compared to the Klems data (Fig. 6), Tensor Tree data include the variable resolution basis, offering higher resolution data where needed (at sharp peaks) and lower resolution data where the BSDF is relatively constant (Fig. 7).

For the tested prismatic film with fabric glazing unit, the normal incidence $\theta_i = 0$ shows a strong downward specularly-transmitting peak flux with a smaller peak flux upward. By gradually increasing the incident light angle θ_i from 0, the outgoing single specular peak flux moves closer to the glazing itself horizontally and turn into peak redirected flux above the horizontal plane at the incident angle of around 25°.

2.3 Field measurements of space illuminance

The field measurement spots grids at the Suming Building ground floor are illustrated in Fig. 8. The measurements grids were set according to the Method of Daylighting Measurements GB/T5699-2008 (Standardization Administration 2008). Along the A-a axis to the F-f axis, two typical sections were set up. B-b, D-d, and F-f axes were along in the middle line of the windows, while A-a, C-c, and E-e axes were along in the middle line of walls between windows, so that the impact

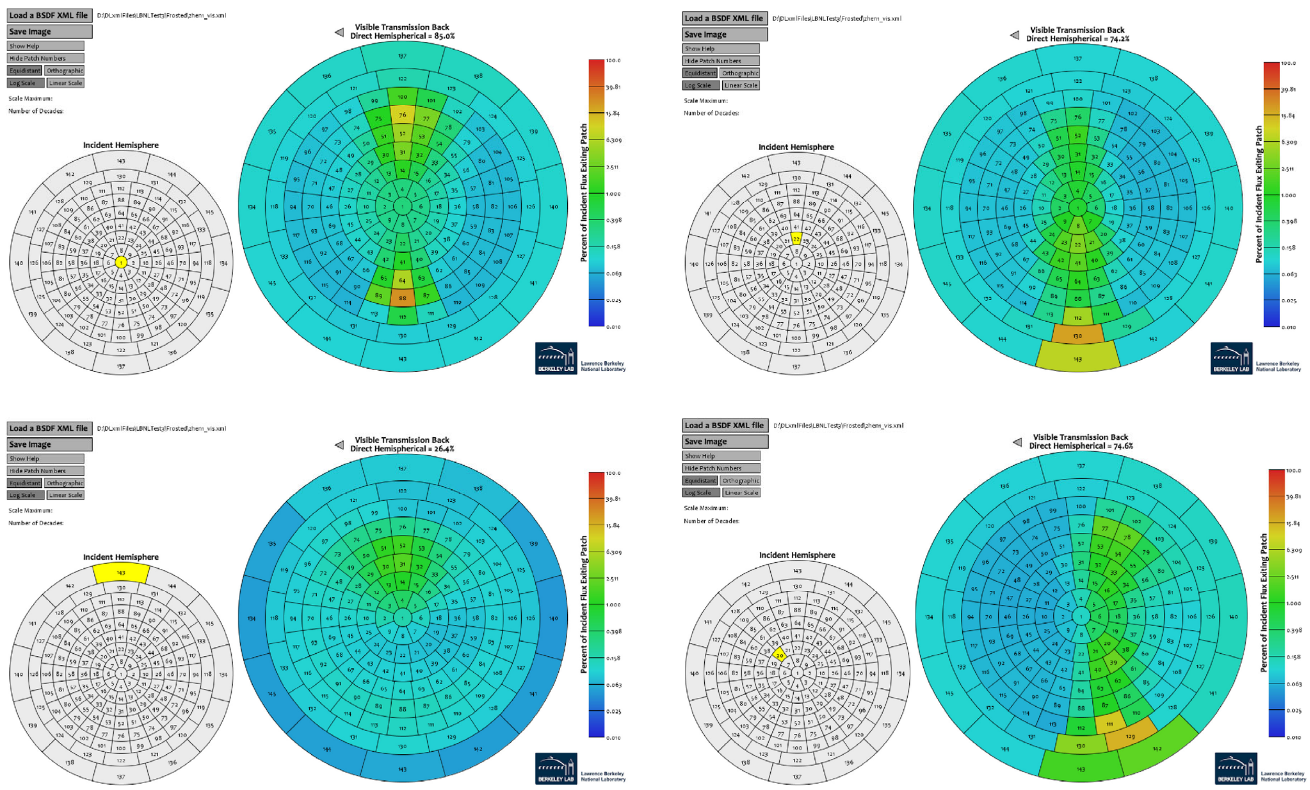

Fig. 6 Incident light and outgoing flux scattering distribution for prismatic film plus fabric glazing (Klems data)

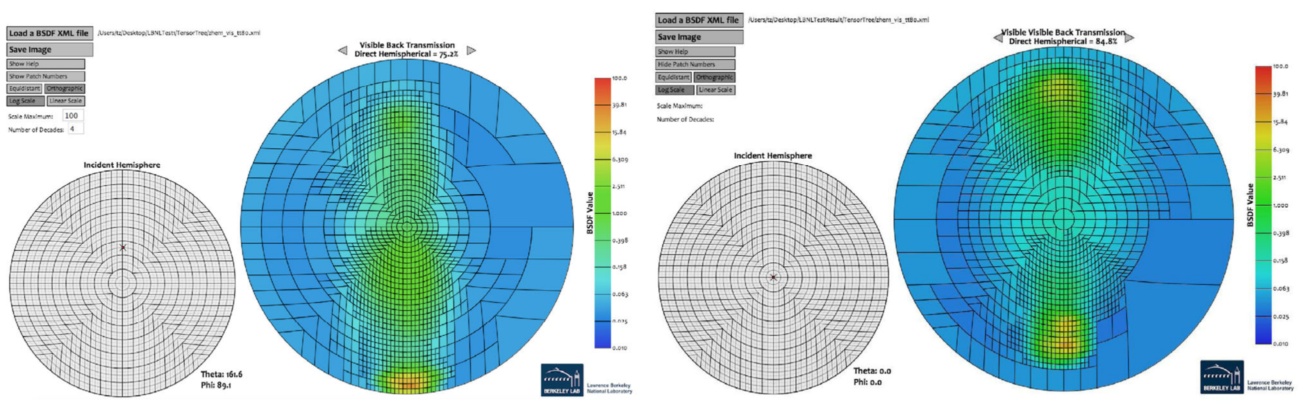

Fig. 7 Incident light and outgoing flux scattering distribution data (Tensor Tree data)

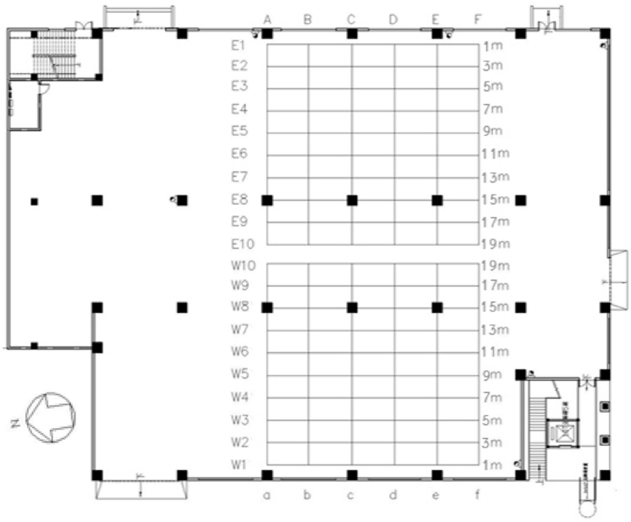

Fig. 8 Illuminance field measurement spots grid

from walls and columns can be taken into account. The illuminance values were measured with a Konica Minolta T-10 illuminance meter (Range 0.01 lx – 300 klx, Accuracy of ±2%) and sequenced along the east-west axes, one spot after another, then one axis after another, to reduce the outdoor illuminance variation impact. Some measurements spots fell in the places where the building columns were located and no measurements were taken at these spots (E8 and W8).

Transverse field measurements of indoor illuminance levels were conducted on the typical days in the summer, autumn and winter seasons. To avoid possible interruption to factory regular manufacturing activities, the undisturbing E-e and F-f axes spots were selected as the longitudinal measurements spots at the height of 0.8 meters above ground.

2.4 Simulation results

Radiance simulations were conducted and field illuminance measurements data were utilized to calibrate the simulation models, in order to evaluate the luminous environment performance with the prismatic film glazing in the manufacture building. In the Radiance simulation model, customized sky module was utilized. Actual weather data of hourly global radiance, diffuse horizontal radiance and direct beam radiance for Shanghai (latitude 31.2°, longitude 121.4°) were obtained from China Meteorological Administration. The measured weather station location is around 60 kilometres from the case study building site. Figures 9 and 10 presented the field measurement and simulation results at 9:00, 12:00 and 15:00 under both clear and overcast sky conditions. The reflectance of the indoor ceiling, wall, column, floor and outdoor ground were set as 0.8, 0.6, 0.6, 0.2, and 0.1 respectively in the simulation models. In order to obtain the more precise resolution, the Tensor Tree data of the prismatic film glazing BSDF XML file was used in the simulation modeling.

2.4.1 *A comparison between the simulation and measurement illuminance data*

The comparison between simulated and measured illuminance levels along the E-e and F-f axes are presented in Figs. 9 and 10. Except for few measurement spots, generally, the simulated illuminance levels with Radiance shows a good match with field measured illuminance data under the clear sky with sun conditions on a typical summer day of July 8.

At around 9:00 under the clear sky with sun, the illuminance levels at east side decrease from around 1900 lx from close to the east side wall to 320 lx along the F-f axis, and decrease from around 1300 lx to 280 lx along the E-e axis, affected by the exterior walls and columns mainly. On

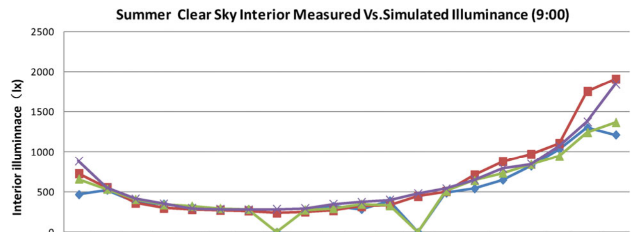

	1m W1	3m W2	5m W3	7m W4	9m W5	11m W6	13m W7	15m W8	17m W9	19m W10	19m E10	17m E9	15m E8	13m E7	11m E6	9m E5	7m E4	5m E3	3m E2	1m E1
Mea.E-e	468	525	374	350	314	289	283	0	272	320	285	390	0	489	542	650	825	1037	1300	1213
Mea.F-f	729	555	363	300	284	274	267	241	254	270	320	334	445	507	713	880	970	1106	1752	1909
Sim.E-e	663	537	408	342	324	296	286	0	277	297	349	331	0	513	643	736	846	948	1243	1367
Sim.F-f	887	553	414	353	299	287	279	287	296	349	373	401	480	541	653	794	850	1070	1374	1845

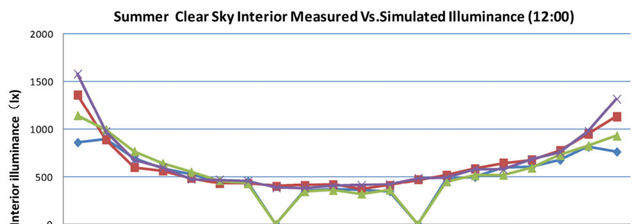

	1m W1	3m W2	5m W3	7m W4	9m W5	11m W6	13m W7	15m W8	17m W9	19m W10	19m E10	17m E9	15m E8	13m E7	11m E6	9m E5	7m E4	5m E3	3m E2	1m E1
Mea.E-e	860	900	692	592	524	446	452	0	351	368	363	345	0	477	498	600	608	676	814	762
Mea.F-f	1360	890	602	565	488	430	427	401	410	420	374	410	470	518	585	645	679	776	950	1130
Sim.E-e	1142	994	765	640	550	461	428	0	346	358	320	361	0	449	515	520	594	726	826	929
Sim.F-f	1580	974	681	597	475	469	454	383	382	407	412	422	486	493	583	578	683	757	978	1316

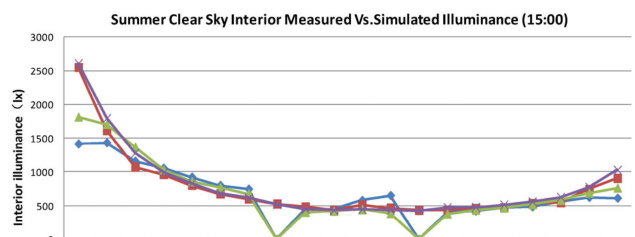

	1m W1	3m W2	5m W3	7m W4	9m W5	11m W6	13m W7	15m W8	17m W9	19m W10	19m E10	17m E9	15m E8	13m E7	11m E6	9m E5	7m E4	5m E3	3m E2	1m E1
Mea.E-e	1413	1432	1158	1054	922	800	745	0	446	442	578	651	0	393	420	472	483	556	623	612
Mea.F-f	2548	1612	1070	960	801	675	600	525	483	430	510	464	432	435	460	468	532	545	740	903
Sim.E-e	1811	1704	1369	1029	854	770	677	0	401	417	442	384	0	377	433	467	518	580	688	762
Sim.F-f	2607	1794	1278	990	830	681	616	516	445	431	445	432	428	474	477	513	558	625	774	1025

*Note: the points with illuminance of 0 are locations of columns

Fig. 9 Measured and simulated illuminance under clear sky for calibrating simulation model

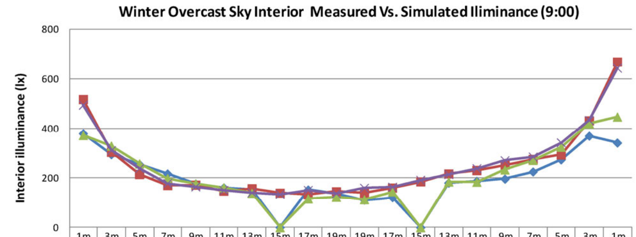

	1m W1	3m W2	5m W3	7m W4	9m W5	11m W6	13m W7	15m W8	17m W9	19m W10	19m E10	17m E9	15m E8	13m E7	11m E6	9m E5	7m E4	5m E3	3m E2	1m E1
Mea.E-e	380	295	255	217	176	161	155	0	152	136	111	121	0	180	187	196	225	274	370	342
Mea.F-f	518	305	215	170	172	148	157	139	132	145	139	160	185	217	231	253	276	294	432	669
Sim.E-e	372	329	257	198	177	161	139	0	116	122	113	144	0	184	184	233	272	325	420	447
Sim.F-f	495	311	239	179	165	151	141	134	151	137	160	164	192	214	239	271	286	343	434	643

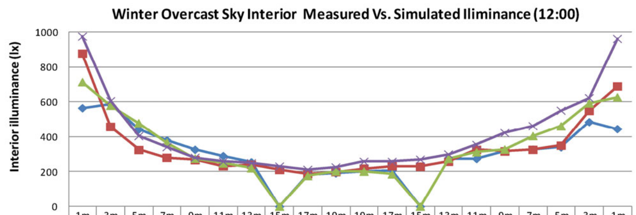

	1m W1	3m W2	5m W3	7m W4	9m W5	11m W6	13m W7	15m W8	17m W9	19m W10	19m E10	17m E9	15m E8	13m E7	11m E6	9m E5	7m E4	5m E3	3m E2	1m E1
Mea.E-e	565	585	442	380	326	290	255	0	184	192	202	209	0	276	274	318	327	340	485	445
Mea.F-f	878	458	325	281	268	233	241	211	188	199	219	233	230	258	326	317	326	350	550	689
Sim.E-e	713	579	479	367	276	249	221	0	176	203	202	186	0	275	312	328	405	462	593	627
Sim.F-f	976	605	404	341	281	259	250	231	212	226	258	258	270	300	354	422	462	551	622	963

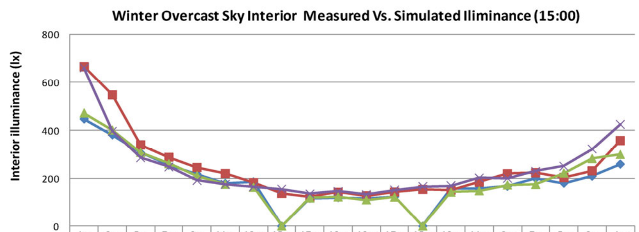

	1m W1	3m W2	5m W3	7m W4	9m W5	11m W6	13m W7	15m W8	17m W9	19m W10	19m E10	17m E9	15m E8	13m E7	11m E6	9m E5	7m E4	5m E3	3m E2	1m E1
Mea.E-e	448	382	307	255	217	179	185	0	117	120	114	123	0	156	159	167	200	180	209	259
Mea.F-f	665	548	340	288	245	220	182	137	122	142	127	143	154	151	184	219	223	203	231	358
Sim.E-e	472	402	308	260	211	175	163	0	118	122	110	121	0	142	148	172	175	222	283	299
Sim.F-f	660	397	285	247	191	175	164	155	135	145	132	152	166	170	201	200	229	250	323	425

*Note: the points with illuminance of 0 are locations of columns

Fig. 10 Measured and simulated illuminance under overcast sky for calibrating simulation model

the west side, the illuminance values decrease from 700 lx to 270 lx and 500 lx to 320 lx, respectively along the F-f and E-e axes. The illuminance difference between east side and west side shows the important impact of the low altitude incident flux in the morning hours. At 12:00, the highest illuminance on the west side is around 1400 lx and is 1100 lx on the east side as the F-f and E-e measurement axes are away from the south walls. The interior illuminance levels are generally over 350 lx even at the locations 19 meters from the walls. At around 15:00, the highest illuminance on the west side is around 2500 lx and indoor illuminance distribution shows a mirror pattern to the 9:00 conditions but with higher illuminance at the positions closer to west walls, as the irradiance is higher at 15:00 than that at 9:00. From the illuminance distribution data, it can also be found that the columns do have impact on the illuminance value of the next measurement spot along the axis from light coming direction.

Under the overcast sky conditions on November 16, the interior illuminance levels are generally below 900 lx without direct sunlight. At 9:00, the illuminance level close to the east walls is around 660 lx, decreasing to around 110 lx at interior space 19 meters from the east walls, and increasing to around 500 lx at locations close to the west walls. At 15:00, interior illuminance levels present a mirrored pattern similar to conditions at 9:00 with illuminance around 350 lx for locations close to the east side walls. At 12:00, the simulated interior illuminance levels are slightly higher than measured data at locations close to the east and west walls. At the locations far away from the walls, the illuminance levels are generally around 200 lx, roughly equivalent to the illuminance levels at 9 meters from the east and west walls at 9:00 or 15:00.

2.4.2 A comparison of the simulation results between prismatic glazing and conventional glazing

With the measured data and calibrated simulation model, a further simulation study was conducted to evaluate the indoor illuminance levels with prismatic film glazing versus those with a conventional glazing. The prismatic film glazing was replaced by a conventional glazing with the visible transmittance of 0.65 in the comparison model. The simulated illuminance levels over the E-e and F-f axes were presented in Table 1 for a clear sky and Table 2 for an overcast sky.

Table 1 shows that, under the clear sky on a typical equinox day of October 14 at 9:00, the exterior direct sunlight is majorly on the east side. The illuminance levels on the east side with the conventional glazing can reach 9000 lx and are much higher than that with the prismatic film glazing; while the results are the opposite at the inner locations away from walls. The illuminance levels at the inner parts were improved with the prismatic film glazing and the illuminance uniformity (U_o) is improved from 0.20 to 0.56.

At 12:00, the illuminance values with the prismatic film glazing are overwhelmingly higher than those with the conventional glazing, except for the points close to the east and west walls. The Uo is improved from 0.34 to 0.5.

At 15:00, the illuminance levels on the west side with the conventional glazing are significantly higher than those with the prismatic film glazing. Simulated data with the conventional glazing shows that the illuminance may reach 15000 lx with direct sunlight and strong solar radiation at the points 3 m from west side windows, while the illuminance is only around 203 lx at the space 17 m from windows. The high illuminance value and strong contrast may cause luminous discomfort and glare issues. The corresponding illuminance uniformity is only 0.09 for the conventional glazing and improved to 0.39 with the prismatic film glazing.

The illuminance values in red color in Table 1 represent the illuminance levels with the prismatic film and higher than those with the conventional glazing at the same points.

Table 1 Illuminance levels (lx) with prismatic and conventional glazing (clear sky)

	Points	W1	W2	W3	W4	W5	W6	W7	W8	W9	W10	E10	E9	E8	E7	E6	E5	E4	E3	E2	E1	
	Distance	1m	3m	5m	7m	9m	11m	13m	15m	17m	19m	19m	17m	15m	13m	11m	9m	7m	5m	3m	1m	U_o
Date 14-Oct 9:00																						
Prismatic glazing	F-f	865	939	760	620	559	529	627	568	546	606	625	640	819	899	983	1031	1218	1322	1563	2069	0.56
	E-e	785	1021	865	646	563	538	480	X	498	499	523	626	X	880	884	886	1000	1201	1452	1470	
Conventional glazing	F-f	881	1008	726	637	520	430	465	366	360	360	433	286	523	642	675	758	1178	1537	2281	9231	0.20
	E-e	802	1084	884	625	558	442	386	X	250	298	338	235	X	479	509	629	958	1353	2253	8815	
Date 14-Oct 12:00																						
Prismatic glazing	F-f	1504	1643	1152	983	819	900	970	882	804	878	855	1108	1285	1394	1447	1588	1624	1657	1895	2305	0.50
	E-e	1616	1796	1351	940	986	814	855	X	598	642	666	802	X	934	1106	1143	1397	1373	1591	1516	
Conventional glazing	F-f	1903	1885	1248	817	749	637	539	526	429	434	556	469	652	764	865	785	1056	1262	1691	2151	0.34
	E-e	1881	2082	1477	1100	807	672	665	X	320	370	303	363	X	494	654	660	880	1057	1379	1583	
Date 14-Oct 15:00																						
Prismatic glazing	F-f	3522	2750	1623	1160	927	691	684	559	538	523	470	552	569	587	614	663	780	778	963	1207	0.39
	E-e	2717	3076	1996	1477	1208	895	990	X	423	397	445	424	X	459	491	511	576	670	789	824	
Conventional glazing	F-f	2440	15003	13874	1075	894	639	486	350	312	371	296	359	399	413	496	662	747	967	1175	1191	0.09
	E-e	1894	14919	14422	1513	1002	867	706	X	203	238	322	237	X	297	383	371	474	669	915	866	

Note: the cells marked as "X"mean there are columns and no measurements were conducted at these points.

Table 2 Illuminance levels (lx) with prismatic and conventional glazing (overcast sky)

	Points	W1	W2	W3	W4	W5	W6	W7	W8	W9	W10	E10	E9	E8	E7	E6	E5	E4	E3	E2	E1	
	Distance	1m	3m	5m	7m	9m	11m	13m	15m	17m	19m	19m	17m	15m	13m	11m	9m	7m	5m	3m	1m	U_o
Date 16-Nov 9:00																						
Prismatic glazing	F-f	495	311	239	179	165	151	141	134	151	137	160	164	192	214	239	271	286	343	434	643	0.47
	E-e	372	329	257	198	177	161	139	X	116	122	113	144	X	184	184	233	272	325	420	447	
Conventional glazing	F-f	814	605	368	231	182	143	125	110	103	93	126	110	156	168	197	312	376	520	724	1032	0.24
	E-e	669	586	391	223	185	150	118	X	76	78	86	83	X	181	169	208	309	464	666	801	
Date 16-Nov 12:00																						
Prismatic glazing	F-f	976	605	404	341	281	259	250	231	212	226	258	270	299	311	354	422	462	551	622	963	0.45
	E-e	713	579	479	367	276	249	221	X	176	203	202	186	X	275	312	328	405	462	593	627	
Conventional glazing	F-f	1659	1206	662	448	304	257	227	169	147	190	192	258	260	300	324	438	577	827	1088	1440	0.21
	E-e	1623	1105	718	548	317	273	257	X	135	117	165	151	X	243	263	381	487	742	1032	1166	
Date 16-Nov 15:00																						
Prismatic glazing	F-f	660	397	285	247	191	175	164	155	135	145	132	152	166	170	201	200	229	250	323	425	0.48
	E-e	472	402	308	260	211	175	163	X	118	122	110	121	X	142	148	172	175	222	283	299	
Conventional glazing	F-f	718	690	474	236	205	197	118	113	86	90	104	115	118	143	176	220	267	375	506	550	0.28
	E-e	567	682	529	355	282	168	163	X	90	77	78	105	X	122	142	183	221	315	408	414	

Note: the cells marked as "X"mean there are columns and no measurements were conducted at these points.

The results indicate that the prismatic film can improve inner spaces illuminance levels under the clear sky with sun.

The illuminance data under an overcast sky on November 16 are presented in Table 2. At 9:00, while the illuminance levels with the prismatic film glazing are lower than the data with the corresponding conventional glazing at the locations close to the east and west walls, the illuminance values with the prismatic film are higher than those with the conventional glazing at the inner space spots. The overall illuminance distribution trend is similar to the illuminance distribution conditions under a clear sky. The illuminance uniformity is also improved from 0.24 to 0.47, but the points of higher illuminance values with the prismatic film glazing are less, compared to the conditions under the clear sky.

At 12:00 and 15:00, the illuminance differences are similar to the 9:00 conditions. Although the illuminance values with the prismatic glazing at spaces within 9 m to windows are lower than the data with the conventional glazing, the illuminance levels at the inner locations 11–20 m from windows are still higher than the illuminance values with the conventional glazing. The overall average illuminance with the prismatic film is lower than that with the conventional glazing.

Tables 1 and 2 indicate that prismatic film glazing daylight systems have better luminous performance on illuminance uniformity in deep-depth manufacture buildings than that with the conventional glazing under clear skies. The systems work less effectively under overcast skies.

2.4.3 Simulation results of prismatic film glazing and conventional glazing in various latitudes

To further investigate the illuminance performance of the prismatic film glazing compared with the conventional glazing, simulations were conducted using the typical weather data for Harbin (latitude 45.7°, longitude 126.7°), Beijing (latitude 39.9°, longitude 116.3°) and Guangzhou (latitude 23.5°, longitude 113.3°). The illuminance levels distribution in summer, autumn, and winter at 9:00, 12:00 and 15:00 for both clear and overcast skies were simulated with the prismatic film glazing and conventional glazing.

The extensive simulation results show generally the similar illuminance distribution profiles as those with the Shanghai weather data. The main difference in illuminance distribution is for the high latitude locations such as Beijing and Harbin in the winter morning hours. As can be seen from Tables 3 and 4, in the early morning at 9:00 for the winter season, the illuminance levels at the inner spaces of the manufacture building with the conventional glazing can reach 2000 lx and 1000 lx for Beijing and Harbin, respectively, while the corresponding illuminance values are only 300 lx and 200 lx with the prismatic film glazing at the same locations. For the spaces close to windows, the illuminance levels with the prismatic film glazing are higher than those with the conventional glazing. The illuminance values present the opposite profile compared with illuminance distribution profiles at other latitude and time period. The reason may be related to the very low altitude sun angle at the high latitude locations (sun altitude 12.7 for Harbin and 12.4 for Beijing) as the direct sun is near perpendicular to the conventional glazing and lighting up the inner spaces. The light scattering features of the prismatic film may reduce this beam radiance effect with the conventional glazing.

The simulated and measured illuminance results indicate that the prismatic film glazing can increase the illuminance levels in inner spaces and reduce illuminance levels for spaces close to windows under both clear and overcast skies, and can improve the overall illuminance uniformity. The results are different from the research from Norwegian University of Science and Technology. In their research, the illuminance levels with the prismatic panel systems are higher in all space zones in summer noon hours under the clear sky, and are lower in all space zones under the overcast sky in a 5.5 m deep test office space, compared to the illuminance levels in a reference room (IEA 2000). The reason may be related to the prismatic panel product properties, latitude, ceiling height, window arrangement differences and etc.

Table 3 Illuminance levels (lx) with prismatic and conventional glazing for winter morning (Beijing)

											Date 20-Dec		9:00									
	Points	W1	W2	W3	W4	W5	W6	W7	W8	W9	W10	E10	E9	E8	E7	E6	E5	E4	E3	E2	E1	
	Distance	1m	3m	5m	7m	9m	11m	13m	15m	17m	19m	19m	17m	15m	13m	11m	9m	7m	5m	3m	1m	U_o
Prismatic glazing	F-f	311	220	163	189	167	184	299	281	298	351	327	417	462	452	619	663	769	929	945	1262	0.38
	E-e	238	218	207	163	178	183	207	X	207	192	225	215	X	421	384	496	606	811	952	1064	
Conventional glazing	F-f	293	267	230	215	2003	208	293	2103	2128	2120	314	2164	2306	2201	394	2347	2430	699	748	660	0.18
	E-e	261	303	249	199	187	183	159	X	205	242	161	227	X	400	2174	2305	497	784	743	535	

Note: the cells marked as “X”mean there are columns and no measurements were conducted at these points.

Table 4 Illuminance levels (lx) with prismatic and conventional glazing for winter morning (Harbin)

											Date 22-Dec		9:00									
	Points	W1	W2	W3	W4	W5	W6	W7	W8	W9	W10	E10	E9	E8	E7	E6	E5	E4	E3	E2	E1	
	Distance	1m	3m	5m	7m	9m	11m	13m	15m	17m	19m	19m	17m	15m	13m	11m	9m	7m	5m	3m	1m	U_o
Prismatic glazing	F-f	392	247	188	176	185	169	203	246	213	266	274	292	338	384	422	458	510	595	731	992	0.46
	E-e	279	249	210	176	156	157	179	X	195	177	191	212	X	323	336	347	420	505	672	707	
Conventional glazing	F-f	423	394	275	212	255	196	975	907	250	1055	1035	1026	1135	1148	1149	1306	1312	1442	975	826	0.22
	E-e	369	424	304	219	283	171	195	X	187	138	161	144	X	248	322	1106	1335	712	909	707	

Note: the cells marked as “X”mean there are columns and no measurements were conducted at these points.

3 Luminous and glare metrics results

In the Suming Decoration Building first floor space, the investigators on site for illuminance measurements noticed glare issues from windows during sunny days, especially at the inner locations away from windows. Further site questionnaires with manufacture workers verified the daylight glare issues within the space.

To evaluate the possible interior discomfort glare conditions, glare index is often utilized. For electric lighting, the CIE 117-1995 Standard, Discomfort Glare in Interior Lighting (CIE 1995), is used as the standard evaluation, which describes the unified glare rating (UGR) formula for small-area (0.0003 to 0.1 steradian) electric light sources. For daylighting, there is no equivalent lighting industry standard. The main two reasons are: (1) daylight glare sources typically have solid angles in excess of 0.1 sr, and (2) the luminous area does not have spatially constant luminance as assumed by CIE 117. Visual glare is being actively investigated by the daylight research community, with organized efforts by the IES Daylight Metrics Committee and CIE Technical Committees. Although there is no widely recognized architectural daylight glare metric that is equivalent to the CIE 117 Unified Glare Rating metric, DGI (daylight glare index) and DGP (daylight glare probability) are in common use daylight glare evaluation index with the latter the relatively better metrics as it accounts for the glare issues from large surfaces such as windows (Wienold and Christoffersen 2006). In this research, both DGI and DGP are utilized in the analysis of possible glare for daylight luminous environment evaluation.

The Radiance simulation of false color luminance image with the prismatic film glazing and a conventional double glazing unit (visible transmittance 0.65) facing east (9:00), south (12:00) and west (15:00) direction are comparatively illustrated in Figs. 11–13. The simulation includes typical days in the summer (July 8), autumn (October 14) and winter seasons (December 12). The statistics of hourly DGP and DGI for the three typical days are presented in Table 5. In the table, the glare metrics DGP and DGI values higher than 0.35 (DGP) and 26 (DGI) are marked as red, representing possible discomfort glares at these moments.

In the morning hours in July, the DGP and DGI with the prismatic film glazing are lower than those with the conventional glazing, even though the luminance values within the vision sight are higher. In the afternoon, the conventional glazing produces similar luminance and glare index to the case of the prismatic glazing. The false color luminance images in the morning and afternoon with the prismatic film glazing show significant differences with those of the conventional glazing. Due to the highly directional scattering and peak flux existing patch properties and reflection grating effects with the prismatic film glazing, the high luminance area within window glazing is much smaller, compared with the conventional glazing, which has large high luminance area and more suitable for using DGP glare metric for evaluation.

In October, at 15:00 the glare metrics of DGP and DGI show the highest values for both the prismatic and conventional glazing. The false color luminance images with the prismatic and conventional glazing present different

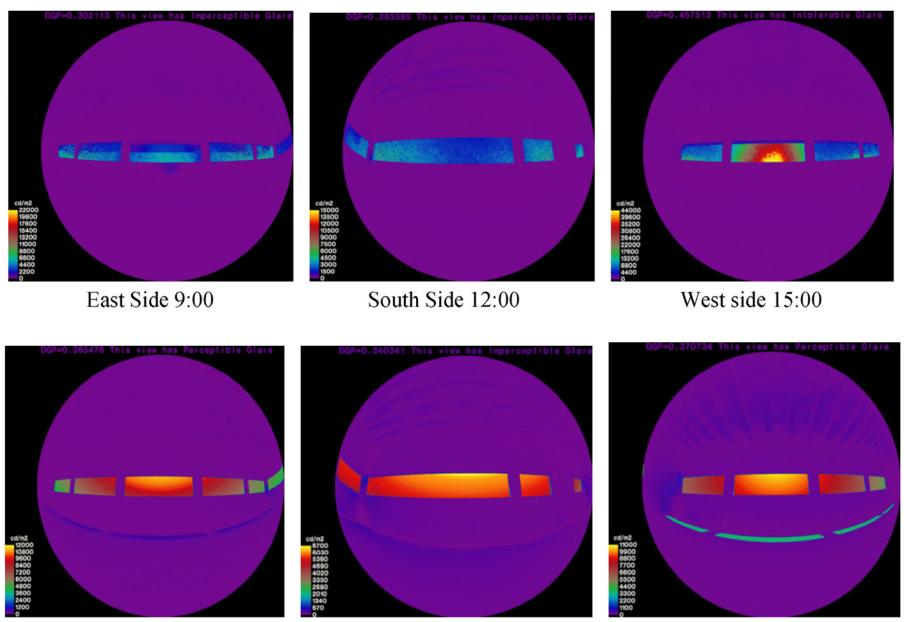

Fig. 11 Summer luminance false color images comparisons

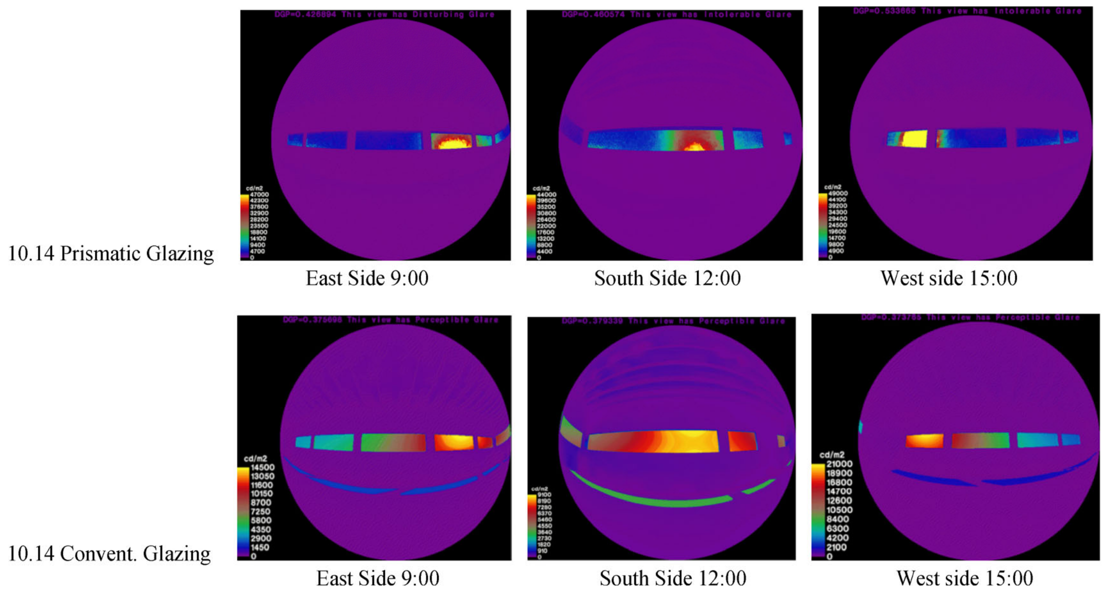

Fig. 12 Autumn luminance false color images comparisons

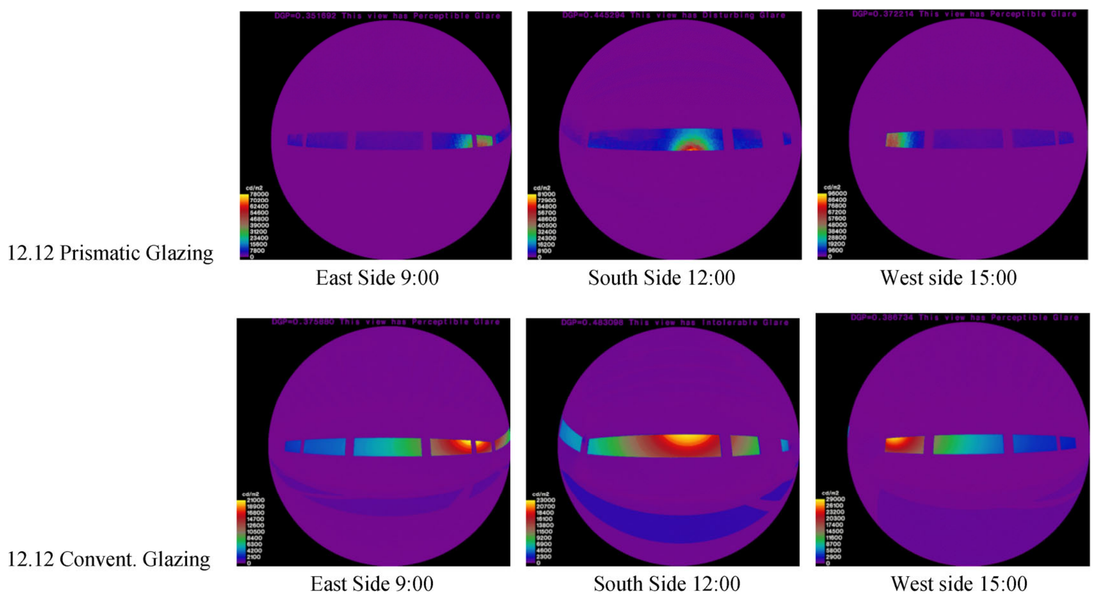

Fig. 13 Winter luminance false color images comparisons

patterns. The glare metrics with the prismatic film glazing are overwhelmingly higher than those with the conventional glazing, except for the early morning and late afternoon.

In December, the glare metrics of DGP with the prismatic film glazing are lower than those with the conventional glazing, while the DGI index is higher around noon hours. The highest DGP and DGI glare metrics occur at around 16:00 for the conventional glazing. At this time the low altitude sun to the west side glazing may cause glare within direct vision views.

From Table 5, it can be seen that even with higher luminance values within direct visions, the statistics of glare metrics of DGP and DGI with the prismatic film glazing are lower than those of the conventional glazing. Except for the autumn/spring season for noon (south orientation) and afteroon hours (west orientation), the DGP and DGI glare metrics with the prismatic film glazing are lower than those with the conventional glazing in a deep-depth facatory building with high sill windows and high ceilings. In the table, the DGI metrics with the conventional glazing are basically almost all exceed 26 and fall into the discomfort glare to intolerable glare categories. This indicates DGI glare metrics may over-estimate the glare conditions with large glare sources such as large windows.

Table 5 Luminance and glare metrics for the simulated prismatic and conventional glazing

			Prismatic glazing			Conventional glazing		
Date	Time	Orientation	Max. luminance	DGP	DGI	Max. luminance	DGP	DGI
7.8	8:00	East	4,300	0.26	23.2	2,800	0.28	25.3
7.8	9:00	East	22,000	0.30	25.7	12,000	0.37	28.2
7.8	10:00	East	28,000	0.30	25.8	8,500	0.35	27.8
7.8	11:00	South	21,000	0.28	23.6	7,300	0.35	27.1
7.8	12:00	South	15,000	0.28	24.5	6,700	0.34	26.7
7.8	13:00	South	11,000	0.27	23.3	5,200	0.33	26.4
7.8	14:00	West	33,000	0.33	26.0	7,700	0.34	27.3
7.8	15:00	West	44,000	0.46	29.4	11,000	0.37	27.9
7.8	16:00	West	43,000	0.39	28.4	25,000	0.45	29.4
7.8	17:00	West	7,200	0.27	23.7	5,500	0.30	26.3
10.14	8:00	East	25,000	0.30	25.7	18,000	0.37	28.5
10.14	9:00	East	47,000	0.43	30.4	14,500	0.38	27.7
10.14	10:00	East	49,000	0.34	27.7	9,500	0.35	27.8
10.14	11:00	South	41,000	0.38	27.6	11,000	0.39	27.4
10.14	12:00	South	44,000	0.46	29.4	9,100	0.38	27.3
10.14	13:00	South	47,000	0.42	28.5	11,000	0.37	26.2
10.14	14:00	West	64,000	0.39	28.7	14,000	0.35	27.8
10.14	15:00	West	49,000	0.53	32.2	21,000	0.37	28.0
10.14	16:00	West	32,000	0.34	26.2	31,000	0.41	28.8
10.14	17:00	West	13,000	0.27	23.6	15,000	0.34	28.3
12.12	8:00	East	17,000	0.26	23.3	15,000	0.33	27.9
12.12	9:00	East	78,000	0.35	28.4	22,000	0.38	28.4
12.12	10:00	East	49,000	0.36	28.6	17,000	0.36	28.3
12.12	11:00	South	59,000	0.45	31.1	24,000	0.48	28.4
12.12	12:00	South	81,000	0.45	31.3	23,000	0.48	28.2
12.12	13:00	South	80,000	0.43	30.6	25,000	0.48	28.3
12.12	14:00	West	61,000	0.31	26.4	15,000	0.35	27.7
12.12	15:00	West	96,000	0.37	29.4	29,000	0.39	27.6
12.12	16:00	West	29,000	0.29	25.1	21,000	0.81	38.8
	Minimum		4,300	0.26	23.2	2,800	0.28	25.3
	Maximum		96,000	0.53	32.2	31,000	0.81	38.8
	Mean		39,584	0.36	27.2	14,904	0.38	27.9
	Median		43,000	0.34	27.6	14,000	0.37	27.6

4 Conclusions

This paper introduced the properties of a prismatic film glazing daylight system and its luminous environment performance in a deep depth manufacture building. Daylight redirecting components such as prismatic film glazing systems are characterized by complex transmissive and reflective behavior that is difficult to predict accurately, due mostly to their highly directional scattering properties and the caustics this produces. Using the bidirectional scattering distribution function (BSDF) method can provide a solution to study the light scattering and distribution properties with the prismatic film glazing.

With the goniophotometric measurements results of light scattering and distribution properties for the prismatic film glazing, simulation with Radiance was conducted to evaluate the luminous environment performance with prismatic film glazing. Illuminance distribution data in the case study large depth manufacture building through field measurements were collected under both clear and overcast skies and used for comparing to corresponding Radiance simulation results with actual weather data from national weather stations, and were also utilized to calibrate the simulation models. The research shows that with laboratory measured light scattering and distribution properties and customized sky with irradiance data, the Radiance simulation values presented a good agreement with the measured illuminance data.

Simulated illuminance data with the prismatic film glazing were compared with illuminance data with the conventional glazing to evaluate the illuminance performance. The comparison of illuminance distribution and values indicated that the prismatic film glazing can provide better illuminance levels at inner areas and overall improved illuminance uniformity for the whole space in large depth buildings such as manufacture spaces under clear skies. The high peak illuminance values at close-to-window locations with conventional glazing under sunny sky may be largely reduced with the prismatic film glazing at side windows, providing less glare and thermal discomfort environment for occupants at these locations. Under an overcast sky, simulation values with the prismatic film glazing presented similar patterns as to those under a clear sky, but with reduced higher illuminance values range at the inner spaces. Meanwhile, even the illuminance uniformity is higher with the prismatic film glazing under the overcast sky, the average illuminance levels with the prismatic film glazing are lower than those with the conventional glazing, indicating a dimmer luminous environment.

Luminance data with the prismatic film and conventional glazing were also analysed, and glare metrics of DGP and DGI within direct view facing side windows were calculated within the Radiance simulation package. The angle-dependent transmittance and reflectance properties of light-scattering for the prismatic film with direct sunlight present a different luminance image pattern from the conventional glazing. While the conventional glazing with direct sunlight may often bring glare issues with large glazing surfaces, the luminance image with the prismatic film with direct sunlight usually has much smaller high luminance areas but much higher luminance values which are often caused by outgoing strong downward specularly-transmitting peak flux of the prismatic film glazing. The glare metrics comparison between the prismatic film glazing and the conventional glazing indicates that although the prismatic film glazing may have higher maximum luminance within vision view, the calculated glare metrics and of DGP and DGI as well as statistics (maximum, minimum, mean and median values) are lower than the corresponding glare metrics with the conventional glazing.

The calculated DGI glare metrics with the conventional glazing basically all fall into discomfort glare range, indicating the DGI glare metrics may overestimate the real glare conditions and may not suit for evaluating glare issues with the conventional glazing. Meanwhile, the DGP glare metrics with the prismatic film indicate that special attentions need to be paid to possible glare occurrence times at summer afternoon for the west side glazing, spring/autumn season noon and afternoon hours for the south facing glazing, as well as winter season noon hours for the south facing glazing. The possible reasons may be related to low altitude sun angles and strong beam solar radiations. As few real-site glare issues instigation with the prismatic film glazing was conducted, further studies may be needed to study the applicability and reliability of the DGP glare metrics for the prismatic film glazing.

Acknowledgements

The project is supported by the Jiangsu Nature Science Research Funding (SBK2016021215), the MOHURD Science and Technology Research Project (2017-K1-010), and Suzhou Municipal Research Funding (SS201730).

References

3M (2017). Daylight redirect film. Available at https://multimedia.3m.com/mws/media/1209715O/3m-daylight-redirecting-film.pdf. Accessed 10 Jul 2017.

Andersen M, Rubin M, Scartezzini J-L (2003). Comparison between ray-tracing simulations and bidirectional transmission measurements on prismatic glazing. *Solar Energy*, 74:157–173.

Andersen M (2004). Innovative bidirectional video-goniophotometer for advanced fenestration systems. PhD Thesis. E′cole polytechnique f ′ed′erale de Lausanne, Switzerland.

Asmail C (1991). Bidirectional Scattering Distribution Function (BSDF): A systematized bibliography. *Journal of Research of the National Institute of Standards and Technology*, 96(2): 215–223.

Beltrán LO, Lee ES, Selkowitz SE (1997). Advanced optical daylighting systems: Light shelves and light pipes. *Journal of the Illuminating Engineering Society*, 26(2): 91–106.

CIE (1995). Discomfort glare in interior lighting, CIE 117-1995. International Commission on Illumination.

Heschong Mahone Group (2003). Windows and Offices: A Study of Office Work Performance and The Indoor Environment. Sacremento CA, USA: California Energy Commission.

IEA (2000). Daylight in Buildings: A Source Book on Daylighting Systems and Components. International Energy Agency Energy.

Klems JH (1994a). A new method for predicting the solar heat gain of complex fenestration systems: I. Overview and derivation of the matrix layer calculation. *ASHRAE Transactions*, 100 (1): 1065–1072.

Klems JH (1994b). A new method for predicting the solar heat gain of complex fenestration systems: II. Detailed description of the matrix layer calculation. *ASHRAE Transactions*, 100 (1): 1073–1086.

LBNL (2017). BSDFViewer, Version1.2. Available at https://www.radiance-online.org/download-install/third-party-utilities/bsdf-viewer. Accessed 10 Jul 2017.

Mashaly IA, Nassar K, El-Henawy SI, Mohamed MN, Galal O, Darwish A, Hassan ON, Safwat AME (2017). A prismatic daylight redirecting fenestration system for southern skies. *Renewable Energy*, 109: 202–2012.

McNeil A, Jonsson J, Appelfeld D, Ward G, Lee E (2013). A validation of a ray-tracing tool used to generate bi-directional scattering distribution functions for complex fenestration systems. *Solar Energy*, 98: 404–414.

McNeil A, Lee E, Jonsson J (2017). Daylight performance of a microstructured prismatic window film in deep open plan offices. *Building and Environment*, 113: 280–297.

RETROSolar (2014). RETROLux. Available at http://www.retrosolar.de/flash/ani_rlux_e.html. Accessed 25 Feb 2014.

Scartezzini J-L, Courrct G (2002). Anidolic daylighting systems. *Solar Energy*, 73:123–135.

Standardization Administration (2008). Method of Daylighting Measurements, GB/T5699-2008. Beijing: Standards Press of China. (in Chinese)

Thanachareonkit A, Scartezzini J-L (2010). Modelling Complex Fenestration Systems using physical and virtual models. *Solar Energy*, 84: 563–586.

Ward G, Mistrick R, Lee E, McNeil A, Jonsson J (2011). Simulating the daylight performance of complex fenestration systems using bidirectional scattering distribution functions within Radiance. *Leukos*, 7: 241–261.

Wienold J, Christoffersen J (2006). Evaluation methods and development of a new glare prediction model for daylight environments with the use of CCD cameras. *Energy and Buildings*, 38: 734–757.